

Shape-Memory Alloys: Effective 3D Modeling, Computational Aspects, Analysis of Actuator and Biomedical Devices

F. Auricchio^{1,2*}, J. Arghavani⁴, M. Conti¹, S. Morganti¹, A. Reali¹, U. Stefanelli³

¹ Dipartimento di Meccanica Strutturale, Università di Pavia, Pavia, Italy

² Center for Advanced Numerical Simulation (CeSNA), IUSS, Pavia, Italy

³ Istituto di Matematica Applicata e Tecnologie Informatiche CNR, Pavia, Italy

⁴ Department of Mechanical Engineering, Sharif University of Technology, Teheran, Iran

* email: auricchio@unipv.it

Abstract:

The employment of shape memory alloys (SMA) in a large number of engineering applications, among which actuators and biomedical devices, has been the motivation for an increasing interest toward a correct and exhaustive modeling of SMA macroscopic behavior in order to construct reliable simulation tools. In this work we use a three-dimensional model, with a good overall description of pseudo-elastic and shape memory behaviors as well as extremely robust solution algorithm, to perform the analysis of SMA micro-actuators and biomedical stent devices. Application of the developed computational tool in simulation of several SMA devices motivates it as an effective tool that can be successfully used in the design, analysis and optimization procedures of SMA devices.

Keywords: shape memory alloy, simulation, biomedical applications, SMA device, micro-gripper, SMA actuator

1. Introduction

Smart or functional materials exhibit special properties that make them a suitable choice for industrial applications in many branches of engineering. Among different types of smart materials, shape memory alloys (SMAs) have unique features known as pseudo-elasticity (or super-elasticity), one-way and two-way shape memory effects. The origin of these material features is the reversible thermo-elastic martensitic phase transformation between a high symmetry, usually cubic, austenitic phase and a low symmetry martensitic phase.

Today, superelastic Nitinol is a common and well-known engineering material in the medical industry. In this work we use a three-dimensional model, giving a good overall description of pseudo-elastic and shape memory behaviors (both in the small-strain [1] and in the finite-strain version [2]), stressing that it is possible to derive not only interesting theoretical considerations (recasting the problem within the framework of the energetic formulation of rate-independent processes and investigating existence and continuous issues at both the constitutive relation and quasi-static evolution level [3]) but also extremely robust solution algorithms [1-2].

We exploit such a constitutive and algorithmic framework in the analysis of SMA micro-actuators and biomedical stent devices with the aim of showing the potential of developed computational

tools in providing a virtual engineering tool in design, analysis, optimization and simulation of SMA devices.

For the simulations, we have implemented the developed constitutive model in a user defined subroutine UMAT in the nonlinear finite element software ABAQUS/Standard.

2. Simulation of SMA devices

In this section, we use the developed computational tool in simulation of four SMA devices. We selected these devices to cover a variety of applications as well as different SMA behaviours. We have used the constitutive model in [1,2] and the following material properties for the simulations:

Table 1: Material parameters for the simulations

Simulation label	2.1	2.2	2.3.1	2.3.2
E [GPa]	51.7	53	51.7	53
ν [-]	0.3	0.3	0.3	0.33
h [MPa]	750	1000	707	1000
β [MPaK ⁻¹]	5.6	2.5	5.33	6.1
T ₀ [°C]	-25	-25	-28	-30
ϵ_L [%]	7.5	4	7.7	5.6
R [MPa]	140	60	141	100

2.1 SMA helical spring actuator

We simulate a helical spring (with a wire diameter of 4 mm, a spring external diameter of 24 mm, a pitch size of 12 mm and with two coils and an initial length of 28 mm) at two different temperatures. An axial force is applied to one end of the helical spring while the other end is completely fixed. The force is increased from zero to its maximum value and unloaded back to zero. Fig. 1 shows the spring initial geometry, the adopted mesh and the deformed shape under the maximum force. After unloading, the spring recovers its original shape as it is expected in the pseudo-elastic regime. Fig. 2 shows the force-displacement diagram. It is observed that the spring shape is fully recovered after load removal. We also simulate the same spring in the case of one-way shape memory effect, in this case after unloading, the spring does not recover its initial shape (Fig. 3), but after heating, its can be recovered. Fig. 4 shows the force-displacement-temperature behaviour.

We now investigate two-way shape memory effect and consider the spring fixed at the top end, initially loaded by a vertical force at the bottom end (Fig. 5A) and then, keeping constant the load, subjected to temperature cycle (Figs. 5 B,C,D). Fig. 6 shows the loading history during the simulation, while Fig. 7 shows the displacement versus temperature.

2.2 SMA micro-gripper

We now simulate the SMA micro-gripper shown in Fig. 8. The micro-gripper geometry is similar to that reported by Kohl (2004) [4] and it has two parts: the upper part (gear actuator) and the lower part (linear actuator). After laser cutting (Fig. 8a), a pre-deformation of 2 mm is applied to the linear actuator, while heating the gear one (Fig. 8b). From now on, at each time, one actuator is martensitic while another one is austenitic. We now heat the linear actuator to a temperature of $T=30$ °C while cooling the gear one to a temperature of $T=-25$ °C which closes the gripper (Fig. 8c). If we then heat the gear actuator and cool down the linear one, the gripper would open again (Fig. 8d). Fig. 9 shows the micro-gripper when it grips a micro-sample.

2.3 SMA biomedical stent

Cardiovascular diseases (CVDs) are the main cause of death in Western countries having a huge economical and social impact. CVDs are often related to atherosclerosis, a degeneration of the vessel wall narrowing the lumen and consequently reducing or blocking the blood flow. An interventional option to reduce such a stenosis is to apply a metallic mesh, called stent, having the goal

to maintain the vessel open. Currently the use of SMA (i.e. Nitinol) to manufacture stents is increasing mainly for peripheral applications where super-elasticity enhance the device features.

Finite element analysis (FEA) has shown to be a very useful tool in the investigation and optimization of stent design, also providing novel insights on fatigue/fracture mechanics. Moreover, given the miniaturized nature of such devices, the performance of experimental tests is not trivial and simulations can be useful tools to speed up the design.

For these reasons, we investigate the behavior of a pseudo-elastic stent and its relative impact on the vessel. We firstly focus on the lonely device performing a virtual bending test; then we perform the simulation of stent implant in a narrowed vessel.

2.3.1 Simulation of stent flexibility test

In the following, we perform a FEA in order to assess the flexibility of a Nitinol self-expanding stent in open configuration. We design the numerical test to mimic the approach proposed by Muller-Hulsbeck [5]. We consider a geometry very similar to the tapered XACT stent (Abbott, Illinois, USA) with a structure characterized by tubular-like rings having the main function of sustaining the vessel after stent expansion, and bridging members (links) having the main function of assuring the stent flexibility by allowing mutual rotation between adjacent rings. We impose the stent bending by a displacement (11 mm) along the Y direction of the distal reference point (Fig. 10). The simulation results are in qualitative agreement with experimental results provided in [5].

2.3.2 Simulation of stent implant in a narrowed vessel

The simulation is defined by two steps: crimping of the stent and vessel inflation by a physiological pressure (100 mmHg) and expansion in the vessel. In the first step, we impose a radial displacement to the whole catheter in order to crimp the stent; In the second step, we gradually release the catheter boundary conditions allowing its re-expansion and thus the stent deployment.

Fig. 11 depicts the results of the simulation highlighting the deformed configuration of the stent and of the vessel after the deployment, highlighting the von Mises stress distribution along the stent structure.

3. Conclusions

In this study, we simulated different SMA devices including springs, micro-gripper and medical stents with the aim of providing a computational tool for

design, analysis, optimization and simulation of SMA devices.

4. References

- [1] F. Auricchio, L. Petrini, "A three-dimensional model describing stress-temperature induced solid phase transformations. Part I: solution algorithm and boundary value problems", *International Journal for Numerical Methods in Engineering*, 61, 807-836, 2004.
- [2] J. Arghavani, F. Auricchio, R. Naghdabadi, A. Reali, "On the robustness and efficiency of integration algorithms for a 3D finite-strain phenomenological SMA constitutive model", Submitted for publication.
- [3] F. Auricchio, A. Mielke, U. Stefanelli, "A rate-independent model for the isothermal quasi-static evolution of shape-memory materials", *Mathematical Models and Methods in Applied Sciences*, 18, 125-164, 2008.
- [4] M. Kohl: *Shape Memory Microactuators*, Springer (2004).
- [5] S. Muller-Hulsbeck, P.J. Schafer, N. Charalambous, S.R. Schaffner, M. Heller and T. Jahnke, "Comparison of Carotid Stents: An In-Vitro Experiment Focusing on Stent Design", *J Endovasc Ther.* 16, 168-177, 2009.



Fig. 1: Pseudo-elastic spring: initial and deformed configurations.

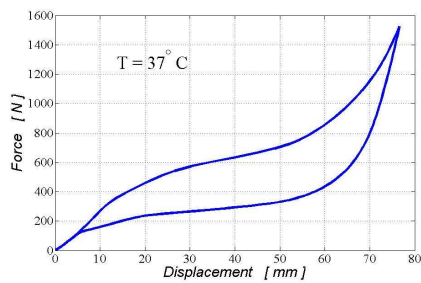


Fig. 2: Force-displacement diagram for the SMA spring: pseudo-elasticity

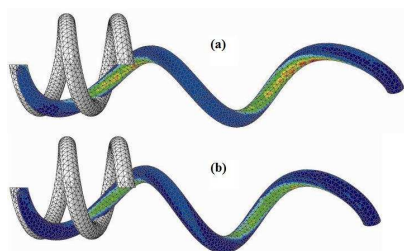


Fig. 3: Shape memory effect: deformed shape a) under maximum load b) after unloading.

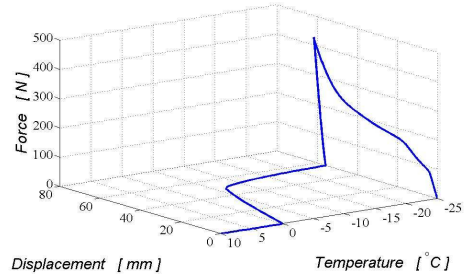


Fig. 4: Force-displacement diagram for the SMA spring: shape memory effect.

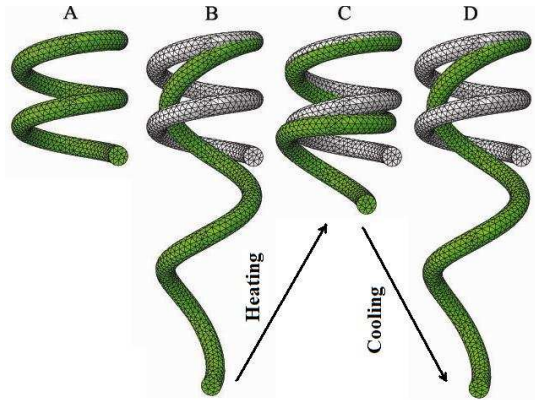


Fig. 5: Spring actuator: A) initial geometry; B) deformed shape due to the weight application at $T = -25$ °C; C) spring shape recovery and weight lifting due to heating to $T = 100$ °C; D) spring stretching due to cooling to $T = -25$ °C.

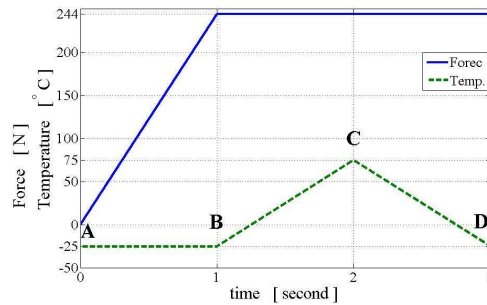


Fig. 6: Loading history during simulation.

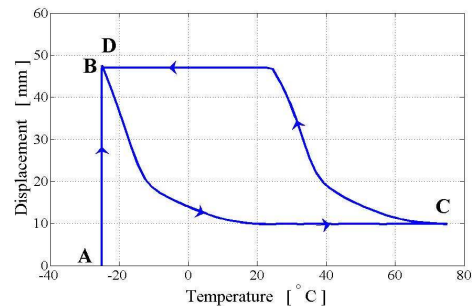


Fig. 7: Vertical displacement of the lower loaded end of spring versus temperature variation.

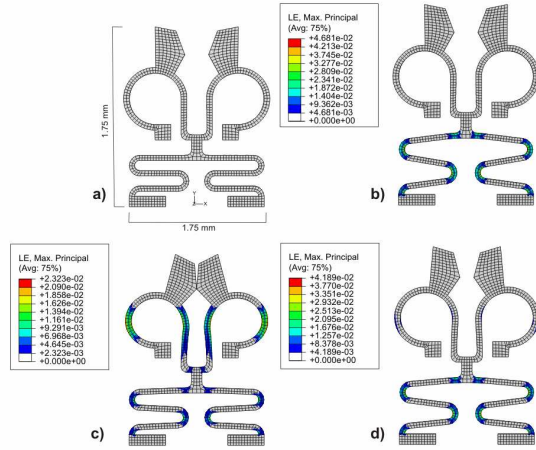


Fig. 8: Finite element analysis of micro-gripper: a) starting configuration; b) memorization step of linear actuator; c) heating of linear actuator and consequent actuation of the gauge; d) heating of gauge actuator with consequent re-opening. Contour plot of maximum principal logarithmic strain is reported.

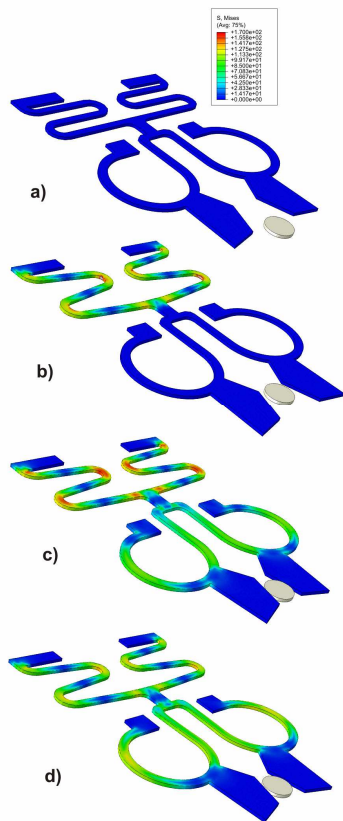


Fig. 9: Simulation of micro-gripper with a sample: a) starting configuration; b) memorization step; c) heating of linear actuator and sample gripping; d) heating of rotary actuator with consequent re-opening. von Mises stress [MPa] distribution in the micro-gripper are depicted in the contour plot.

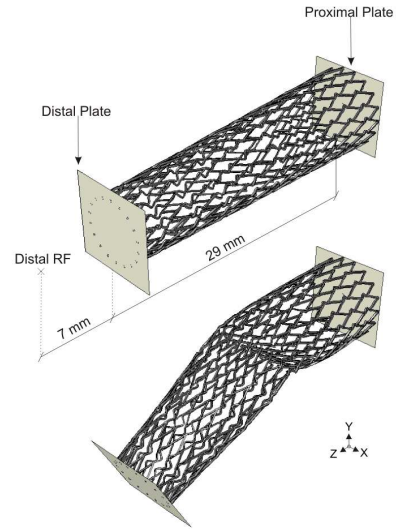


Fig. 10: Flexibility test of Nitinol stent; initial configuration (top); final bent configuration (bottom).

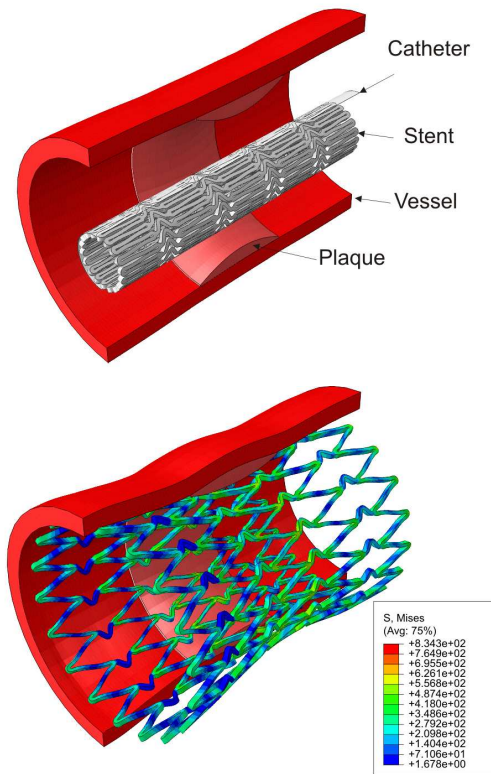


Fig. 11: Simulation of stent implant in a narrowed vessel; stent crimped in the catheter (top); stent delivered in the vessel. Von Mises stress [MPa] distribution in stent after the deployment are depicted in the contour plot (bottom).